

INTEGRATED ACTIVE FIBRES IN VIBRATION CONTROL OF HELICOPTER BLADES

F.F. Afagh*
Carleton University
Ottawa, Canada

Keywords: integrated active fibres, composites, rotor blades, structural modelling, aeroelastic stability

Abstract

A new model has been developed to characterise the structural behaviour of rotor blades that benefit from fully integrated active fibre construction. The beam wall is assumed to consist of a composite laminate with passive as well as active material plies. Standard theory describing the macro-mechanical behaviour of composites is employed to formulate the cross-sectional stiffness matrix and the actuation forces and moments in the rotor blade. The symmetric stiffness matrix and the actuation vector include the effects of axial, shear, bending, torsion and bimoment actions in the rotor blade.

This structural model is used to obtain a non-linear dynamic model for the rotor blade that can be used to investigate the aeroelastic stability of the system or using various individual blade control (IBC) schemes to control the vibration of the rotor blades. Hamilton's principle is used to obtain the corresponding governing differential equations of motion and boundary conditions for a cantilever beam rotating at a constant speed. Galerkin's method can be used to solve the differential equations of motion. This results in a system of linear, homogeneous, constant coefficient, ordinary differential equations that define the unsteady blade motion near the equilibrium operating conditions. These equations can be used to investigate the stability of the motion or control the vibration of the rotors individually by a suitable actuation scheme of the integrated actuators.

1. Structural Modelling of the Rotor Blade

1.1 Introduction

A typical helicopter rotor blade is exposed to a complicated system of unsteady time-dependent aerodynamic loads during its operation. As the consequence, besides being subjected to a bi-axial bending which results from flapping and lead-lag actions a rotor blade is also subjected to torsion and axial centrifugal tension.

Structurally more simple hingeless rotor design is a by-product of the initial impetus for using composites in order to improve the fatigue life and damage tolerance of the blade [1]. Depending on their specific construction, these blades can exhibit various structural couplings between bending, shear, torsion and extension actions. Warping may also become a prominent effect in such advanced blades. Therefore, the Euler-Bernoulli beam assumptions used to model simpler isotropic beams become invalid under these conditions.

Existing theories of mechanics of composite materials can be employed to model the above-mentioned non-classical effects in the rotor blades. To this end, in the present work, a hingeless rotor blade is considered where it is modelled as a closed single cell, thin-walled composite beam. The model assumes a beam wall that is constructed from composite laminae. In general, it allows for different thickness and orientation for each ply that may be constructed of either passive or active fibres. The active laminae can be placed anywhere in the stacking sequence. In view of large length-to-chord ratios of helicopter blades a one-

*Professor, Department of Mechanical and Aerospace Engineering
 Email: fafagh@mae.carleton.ca

dimensional beam model is adopted. The material constitutive relations are determined using the strains that are, in turn, obtained from basic displacement field.

1.2 Displacement Field

The co-ordinate systems used in this study are shown in Fig.(1.1-a). The orthogonal axes system $(X_{\mathcal{F}}, Y_{\mathcal{F}}, Z_{\mathcal{F}})$ are fixed in an inertial frame \mathcal{F} . The global orthogonal co-ordinate system (x, y, z) and associated unit vectors $(\mathbf{i}, \mathbf{j}, \mathbf{k})$ are fixed in a reference frame \mathcal{R} that rotates with respect to \mathcal{F} at constant angular velocity Ω . Point O_0 , a common fixed point of \mathcal{F} and \mathcal{R} is located at the root of the rotor. The x -axis lies along the elastic-axis of the beam that passes through shear centres of all cross sections. As a first attempt, the pre-cone angle is assumed to be zero, and the plane containing $X_{\mathcal{F}}$, x , $Y_{\mathcal{F}}$ and y is considered to be the plane of rotation. The origin O_1 of the local Cartesian co-ordinate system (x, t, n) is located on the mid-plane of the beam wall and moves along the contour with the circumferential co-ordinate s as shown in Fig.(1.1-b). The co-ordinates of O_1 in the global co-ordinate system are denoted as $(X, Y(s), Z(s))$. Moreover, using the normal co-ordinate n to denote the position of any other point P on the beam wall with respect to (x, n, t) , the position of any point on the wall can be completely defined in the global co-ordinate system.

Next, in reference to Figs.(1.1-b) and (1.2), let the following be denoted:

- u, v, w : global displacements of O , in the x , y , and z directions, respectively, representing an average cross-sectional displacement at any distance x along the elastic axis;
- u_p, v_p, w_p : global displacements of any point P on the beam wall in the x , y , z , directions, respectively;
- $\phi(x), \theta_y(x), \theta_z(x)$: cross-sectional rotation about x , y , and z axis, respectively;
- $\phi'(x)$: rate of twist of the beam;

$\psi(s)$: torsional warping of the cross-section.

Then the displacements of a point P on the beam wall can be expressed as follows:

$$u_p = u(x) - (Y - nZ_{,s})\theta_z(x) + (Z + nY_{,s})\theta_y(x) + \psi\phi'(x) \quad (1.1)$$

where $(\)_{,s} \equiv \frac{\partial(\)}{\partial s}$ and

$$\psi(s) = \frac{-2A}{\Gamma} \int_0^s \alpha ds + \int_0^s r_n ds \quad (1.1.1)$$

$$\alpha = \frac{\Gamma / (G_{eff} h)}{\oint_{\Gamma} [1 / (G_{eff} h)] ds} \quad (1.1.2)$$

and,

$$v_p = v(x) - \phi(Z + nY_{,s}) \quad (1.2)$$

$$w_p = w(x) + \phi(Y - nZ_{,s}) \quad (1.3)$$

Where A and Γ represent, respectively, the area and the perimeter of the contour enclosed by the mid-plane of the cross-section, h is the wall thickness and G_{eff} is the effective shear modulus. In Eq.(1.1) the terms $nZ_{,s}\theta_z(x)$ and $nY_{,s}\theta_y(x)$ represent the axial displacement of the point P due to cross-sectional rotations θ_z and θ_y , respectively; while in Eqs.(1.2) and (1.3) the terms $\phi(Z + nY_{,s})$ and $\phi(Y - nZ_{,s})$ represent the displacement components in the y and z directions of point P due to cross-sectional rotation about the x -axis.

1.3 Strain- Displacement Relations

The displacement field obtained in the previous section is used to obtain the necessary strain-displacement relations. To this end, displacements are defined according to the conventional small deformation theory. Hence,

using Eq.(1.1), one gets the axial strain at any point P on the beam wall as:

$$\begin{aligned}\varepsilon_{xx} &= \frac{\partial u_p}{\partial x} = u'(x) - Y\theta'_z(x) + Z\theta'_y(x) \\ &\quad + \psi(s)\phi''(x) + n[Y_{,s}\theta'_y(x) + Z_{,s}\theta'_z(x)] \\ &= \varepsilon_{xx}^\circ + n\kappa_{xx}\end{aligned}\quad (1.5)$$

Where ε_{xx}° and κ_{xx} are the axial strain of the middle-surface and the curvature, respectively. Denoting the displacement along the tangential direction t as v_t , the in-plane shear strain is defined as

$$\gamma_{xs} = \frac{\partial u_p}{\partial s} + \frac{\partial v_t}{\partial x}\quad (1.6)$$

Noting that v_p and w_p contribute to v_t such that

$$v_t = v_p Y_{,s} + w_p Z_{,s}\quad (1.7)$$

plane shear strain across the blade wall thickness, and neglecting higher order terms, one can show that Eq.(1.6) becomes

$$\begin{aligned}\gamma_{xs} &= (v' - \theta_z)Y_{,s} + (w' + \theta_y)Z_{,s} - \frac{2A}{\Gamma}\alpha\phi' \\ &\equiv \gamma_{xs}^\circ\end{aligned}\quad (1.8)$$

which is the expression for the in-plane shear strain γ_{xs}° at the mid-plane. Next, using Eqs.(1.1-1.3), the transverse shear strains (Timoshenko beam shear definition) are identified as:

$$\gamma_{xy} = v' - \theta_z\quad (1.9.1)$$

$$\gamma_{xz} = w' + \theta_y\quad (1.9.2)$$

so that the in-plane shear strain in Eq.(1.8) can be expressed as

$$\gamma_{xs} = \gamma_{xy}Y_{,s} + \gamma_{xz}Z_{,s} - \frac{2A}{\Gamma}\alpha\phi'\quad (1.10)$$

1.4 Constitutive Relations

The standard theory describing the macro-mechanical behaviour of composites is used in the following deliberation [2]. Moreover, any material non-linearity is assumed to be absent in both the active and passive materials of the composite, and therefore, the linear piezoelectric constitutive equations can be used. Also, in view of the fact that electrical

displacements will not be of the main interest in actuation of the rotor blade, the only constitutive equation that needs to be considered is

$$\mathbf{T} = \mathbf{c}^E \mathbf{S} - \mathbf{e}^T \mathbf{E} = \mathbf{c}^E \mathbf{S} - [\mathbf{d} \mathbf{c}^E]^T \mathbf{E}\quad (1.11)$$

In conventionally poled piezoelectric the poled direction is assigned to be the 3-axis with the (1-2)-plane being the plane of isotropy. However, for passive fibres such as carbon or glass fibres as well as the piezoelectric fibres that are to be used in the construction of the rotor blade the corresponding passive and active laminae are transversely isotropic materials along the fibre direction. Therefore, the material 1-axis is assigned to be along the fibre direction for such a construction. As the result the (2-3)-plane becomes the plane of isotropy (for both active and passive fibres), with the poling for active fibres now being in the 1-axis direction, Fig.(1.3). In this co-ordinate system the corresponding constitutive relations for active as well as passive laminae become:

$$\begin{bmatrix} \sigma_{11} \\ \sigma_{22} \\ \sigma_{33} \\ \tau_{23} \\ \tau_{31} \\ \tau_{12} \end{bmatrix} = \begin{bmatrix} C_{11} & C_{12} & C_{12} & 0 & 0 & 0 \\ C_{12} & C_{22} & C_{23} & 0 & 0 & 0 \\ C_{13} & C_{23} & C_{22} & 0 & 0 & 0 \\ 0 & 0 & 0 & \frac{C_{22} - C_{23}}{2} & 0 & 0 \\ 0 & 0 & 0 & 0 & C_{66} & 0 \\ 0 & 0 & 0 & 0 & 0 & C_{66} \end{bmatrix}^E \begin{bmatrix} \varepsilon_{11} \\ \varepsilon_{22} \\ \varepsilon_{33} \\ \gamma_{23} \\ \gamma_{31} \\ \gamma_{12} \end{bmatrix} - \begin{bmatrix} e_{11} \\ e_{12} \\ e_{13} \\ 0 \\ 0 \\ 0 \end{bmatrix} E_1\quad (1.12)$$

with the engineering shear strains and tensor shear strains defined as ($ij = 2, ij$, for $i \neq j$). For passive fibres $E_1 = 0$.

For a closed thin-wall beam the normal stresses in the thickness direction as well as the longitudinal and transverse shear stresses in the wall are considered to be negligible, i.e., by setting $\sigma_{33} = \tau_{23} = \tau_{31} = 0$ in Eqs.(1.12) a plane stress state is defined. Hence, applying a static condensation to Eqs.(1.12), the constitutive relations for the orthotropic material in a plane stress state are obtained as:

$$\begin{bmatrix} \varphi_1 \\ \varphi_2 \\ \varphi_2 \end{bmatrix} = \begin{bmatrix} Q_{11} & Q_{12} & 0 \\ Q_{12} & Q_{22} & 0 \\ 0 & 0 & Q_{66} \end{bmatrix} \begin{bmatrix} \xi_1 \\ \xi_2 \\ \gamma_{12} \end{bmatrix} - \begin{bmatrix} e_{11}^p \\ e_{12}^p \\ 0 \end{bmatrix} E_1\quad (1.13)$$

where,

$$\begin{aligned} Q_{11} &= C_{11} - \frac{C_{12}^2}{C_{22}}, \quad Q_{12} = C_{12} - \frac{C_{12}C_{23}}{C_{22}}, \\ Q_{22} &= C_{22} - \frac{C_{23}^2}{C_{22}}, \quad Q_{66} = C_{66}, \\ e_{11}^p &= e_{11} - \frac{C_{12}}{C_{22}} e_{13}, \\ e_{12}^p &= e_{12} - \frac{C_{23}}{C_{22}} e_{13}. \end{aligned} \quad (1.14)$$

The plane stress constitutive relations given by Eqs.(1.14) are in reference to the co-ordinate system $(1,2,3)$ which is aligned with the principal fibre directions. To obtain the corresponding relations in the main structural co-ordinate system (x,t,n) , the material properties must be rotated through the proper angle θ , Fig.(1.4), using the standard tensor transformation matrix. The transformed stress-strain relations will read as:

$$\begin{bmatrix} \sigma_{xx} \\ \sigma_{ss} \\ \tau_{xs} \end{bmatrix} = \begin{bmatrix} \bar{Q}_{11} & \bar{Q}_{12} & \bar{Q}_{16} \\ \bar{Q}_{12} & \bar{Q}_{22} & \bar{Q}_{26} \\ \bar{Q}_{16} & \bar{Q}_{26} & \bar{Q}_{66} \end{bmatrix} \begin{bmatrix} \varepsilon_{xx} \\ \varepsilon_{ss} \\ \gamma_{xs} \end{bmatrix} - \begin{bmatrix} e_{1xx} \\ e_{1ss} \\ e_{1xs} \end{bmatrix} E_1 \quad (1.15)$$

where the rotated ply stiffness are

$$\begin{aligned} \bar{Q}_{11} &= U_1 + U_2 \cos 2\theta + U_3 \cos 4\theta \\ \bar{Q}_{12} &= U_4 - U_3 \cos 4\theta \\ \bar{Q}_{16} &= \frac{1}{2} U_2 \sin 2\theta + U_3 \sin 4\theta \\ \bar{Q}_{22} &= U_1 - U_2 \cos 2\theta + U_3 \cos 4\theta \\ \bar{Q}_{26} &= \frac{1}{2} U_2 \sin 2\theta - U_3 \sin 4\theta \\ \bar{Q}_{66} &= U_5 - U_3 \cos 4\theta \end{aligned} \quad (1.16)$$

with

$$\begin{aligned} U_1 &= \frac{3Q_{11} + 3Q_{22} + 2Q_{12} + 4Q_{66}}{8} \\ U_2 &= \frac{Q_{11} - Q_{22}}{2} \\ U_3 &= \frac{Q_{11} + Q_{22} - 2Q_{12} - 4Q_{66}}{8} \\ U_4 &= \frac{Q_{11} + Q_{22} + 6Q_{12} - 4Q_{66}}{8} \\ U_5 &= \frac{Q_{11} + Q_{22} - 2Q_{12} + 4Q_{66}}{8} \end{aligned} \quad (1.17)$$

and the rotated induced stresses are

$$\begin{aligned} e_{1xx} &= e_{11}^p \cos^2 \theta + e_{12}^p \sin^2 \theta \\ e_{1ss} &= e_{11}^p \sin^2 \theta + e_{12}^p \cos^2 \theta \\ e_{1xs} &= (e_{11}^p - e_{12}^p) \sin \theta \cos \theta \end{aligned} \quad (1.18)$$

1.5 Stress Resultants in the Rotor Blade

The stress resultants per unit length around the perimeter of the beam wall are obtained by integrating the stresses given in Eqs.(1.15) across the wall thickness h . To this end, the classical laminated plate theory is invoked first, according to which the strain at any point across the plate thickness can be expressed in terms of the middle-surface strains ε_{ij}^o and curvatures κ_{ij} . Hence, Eqs.(1.15), can be rewritten as

$$\begin{bmatrix} \sigma_{xx} \\ \sigma_{ss} \\ \tau_{xs} \end{bmatrix} = \begin{bmatrix} \bar{Q}_{11} & \bar{Q}_{12} & \bar{Q}_{16} \\ \bar{Q}_{12} & \bar{Q}_{22} & \bar{Q}_{26} \\ \bar{Q}_{16} & \bar{Q}_{26} & \bar{Q}_{66} \end{bmatrix} \begin{bmatrix} \varepsilon_{xx}^o + n\kappa_{xx} \\ \varepsilon_{ss}^o + n\kappa_{ss} \\ \gamma_{xs}^o + n\kappa_{xs} \end{bmatrix} - \begin{bmatrix} e_{1xx} \\ e_{1ss} \\ e_{1xs} \end{bmatrix} E_1 \quad (1.19)$$

Upon integrating these stresses across the wall thickness one gets the following stress resultants:

$$\begin{bmatrix} N_{xx} \\ N_{ss} \\ N_{xs} \\ M_{xx} \\ M_{ss} \\ M_{xs} \end{bmatrix} = \begin{bmatrix} \mathbf{A} & \mathbf{B} \\ \mathbf{B} & \mathbf{D} \end{bmatrix} \begin{bmatrix} \varepsilon_{xx}^o \\ \varepsilon_{ss}^o \\ \gamma_{xs}^o \\ \kappa_{xx} \\ \kappa_{ss} \\ \kappa_{xs} \end{bmatrix} - \begin{bmatrix} N_{xx}^a \\ N_{ss}^a \\ N_{xs}^a \\ M_{xx}^a \\ M_{ss}^a \\ M_{xs}^a \end{bmatrix} \quad (1.20)$$

with extensional, coupling and bending stiffness of, respectively,

$$\begin{aligned} A_{ij} &= \int_{-h/2}^{h/2} \bar{Q}_{ij} dn, & B_{ij} &= \int_{-h/2}^{h/2} n \bar{Q}_{ij} dn, \\ D_{ij} &= \int_{-h/2}^{h/2} n^2 \bar{Q}_{ij} dn, & i,j &= 1,2,6 \end{aligned} \quad (1.21)$$

and stress resultants for actuation forces and moments of

$$\begin{aligned}
 N_{xx}^a &= \int_{-h/2}^{h/2} e_{1xx} E_1 dn, & N_{ss}^a &= \int_{-h/2}^{h/2} e_{1ss} E_1 dn, \\
 N_{xs}^a &= \int_{-h/2}^{h/2} e_{1xs} E_1 dn, \\
 M_{xx}^a &= \int_{-h/2}^{h/2} n e_{1xx} E_1 dn, & M_{ss}^a &= \int_{-h/2}^{h/2} n e_{1ss} E_1 dn, \\
 M_{xs}^a &= \int_{-h/2}^{h/2} n e_{1xs} E_1 dn
 \end{aligned} \quad (1.22)$$

Next, for the rotor blade under consideration, the beam cross-section is assumed as infinitely rigid in its own plane, so that κ_{ss} and κ_{xs} is set equal to zero. Moreover, since the internal pressure of the closed cell beam is equal to the external pressure, the hoop stress σ_{ss} will also vanish so that $N_{ss} = M_{ss} = 0$. Finally, ignoring the edge twist moment resultant M_{xs} , one may apply static condensation to Eqs.(1.20) to obtain the stress resultants for the rotor blade beam as:

$$\begin{bmatrix} N_{xx} \\ N_{xs} \\ M_{xx} \end{bmatrix} = \begin{bmatrix} \bar{A}_{11} & \bar{A}_{12} & \bar{A}_{13} \\ \bar{A}_{12} & \bar{A}_{22} & \bar{A}_{23} \\ \bar{A}_{13} & \bar{A}_{23} & \bar{A}_{33} \end{bmatrix} \begin{bmatrix} \varepsilon_{xx}^\circ \\ \gamma_{xs}^\circ \\ \kappa_{xx} \end{bmatrix} - \begin{bmatrix} \bar{N}_{xx}^a \\ \bar{N}_{xs}^a \\ \bar{M}_{xx}^a \end{bmatrix} \quad (1.23)$$

where,

$$\begin{aligned}
 \bar{A}_{11} &= A_{11} - \frac{A_{12}^2}{A_{22}}, & \bar{A}_{12} &= A_{16} - \frac{A_{12}A_{26}}{A_{22}}, \\
 \bar{A}_{13} &= B_{11} - \frac{A_{12}B_{12}}{A_{22}}, & \bar{A}_{22} &= A_{66} - \frac{A_{26}^2}{A_{22}}, \\
 \bar{A}_{23} &= B_{16} - \frac{A_{26}B_{12}}{A_{22}}, & \bar{A}_{33} &= D_{11} - \frac{B_{12}^2}{A_{22}},
 \end{aligned} \quad (1.24)$$

with the actuation stress resultants

$$\begin{aligned}
 \bar{N}_{xx}^a &= N_{xx}^a - \frac{A_{12}}{A_{22}} N_{ss}^a \\
 \bar{N}_{xs}^a &= N_{xs}^a - \frac{A_{26}}{A_{22}} N_{ss}^a \\
 \bar{M}_{xx}^a &= M_{xx}^a - \frac{B_{12}}{A_{22}} N_{ss}^a
 \end{aligned} \quad (1.25)$$

1.6 Beam Stiffness and Actuation Forces

The internal forces and moments acting over the cross-section of the beam are given as the components of the force vector

$$\mathbf{F}^T = [P_x \quad P_y \quad P_z \quad M_x \quad M_y \quad M_z \quad Q_w] \quad (1.26)$$

with the axial force, P_x , shear forces, P_y, P_z , twisting moment, M_x , lead-lag moment, M_y , flap moment M_z , and bimoment, Q_w defined as

$$\begin{aligned}
 P_x &= \oint_{\Gamma} N_{xx} ds, & P_y &= \oint_{\Gamma} N_{xs} Y_{,s} ds, \\
 P_z &= \oint_{\Gamma} N_{xs} Z_{,s} ds, & M_x &= \oint_{\Gamma} N_{xs} \left(\frac{-2A\alpha}{\Gamma} \right) ds, \\
 M_y &= \oint_{\Gamma} (N_{xx} Z + M_{xx} Y_{,s}) ds, \\
 M_z &= \oint_{\Gamma} (-N_{xx} Y + M_{xx} Z_{,s}) ds, \\
 Q_w &= \oint_{\Gamma} N_{xx} \psi ds,
 \end{aligned} \quad (1.27)$$

where, all the integration is around the beam wall at the mid-plane. The resultant stresses from Eqs.(1.23) are substituted into the expressions given in (1.27), to get

$$\mathbf{F} = \mathbf{K}\mathbf{u} - \mathbf{F}^a \quad (1.28)$$

where the beam stiffness matrix is obtained as

$$\mathbf{K} = \begin{bmatrix} K_{11} & K_{12} & K_{13} & K_{14} & K_{15} & K_{16} & K_{17} \\ & K_{22} & K_{23} & K_{24} & K_{25} & K_{26} & K_{27} \\ & & K_{33} & K_{34} & K_{35} & K_{36} & K_{37} \\ & & & K_{44} & K_{45} & K_{46} & K_{47} \\ & & & & K_{55} & K_{56} & K_{57} \\ & & & & & K_{66} & K_{67} \\ & & & & & & K_{77} \end{bmatrix} \quad (1.29)$$

The expressions for the stiffness coefficients K_{ij} for the normal internal force N are given in the Appendix. Other stiffness coefficients are obtained in a similar fashion, [3]. The global displacements and actuation forces in Eqs.(1.28) are, respectively,

$$\mathbf{u}^T = [u' \quad \gamma_{xy} \quad \gamma_{xz} \quad \phi' \quad \theta_y' \quad \theta_z' \quad \phi''] \quad (1.30)$$

$$[\mathbf{F}^a]^T = [P_x^a \quad P_y^a \quad P_z^a \quad M_x^a \quad M_y^a \quad M_z^a \quad Q_w^a] \quad (1.31)$$

where, the elements of the applied force vector are given in the Appendix.

2 Governing Equations of Motion

2.1 Introduction

Hamilton's principle is used to obtain the governing differential equations of motion and boundary conditions for a cantilever beam rotating at constant speed:

$$\delta\Pi = \int_1^2 (\delta U - \delta T - \delta W) dt = 0 \quad (2.1)$$

The resulting system of non-linear governing equations of motion is expected to be a relatively large and complicated system. Therefore, it would be desirable to neglect higher order terms to reduce the size and complexity of these equations. Such a reduction has to be implemented in a systematic manner if non-selfadjoint operators are to be avoided in the resulting equations. To achieve this, a consistent set of guidelines, parallel to the ones that were used in references [3,4,5] has been adopted in this report. These guidelines are based on introducing a parameter ε that represents the order of the dimensionless flap deflection v/R . Table (2.1) lists the order of magnitudes for various parameters that are used in the present work. In general, in applying this ordering scheme, terms of order ε^2 are ignored with respect to unity.

2.2 Strain Energy Contribution

The variation of strain energy for the thin walled composite beam is

$$\delta U = \int_{\Gamma}^R \int (N_{xx} \delta \varepsilon_{xx}^e + N_{xs} \delta \gamma_{xs}^e + M_{xx} \delta \kappa_{xx}) ds dx \quad (2.2)$$

where, R is the length of the beam. Using the appropriate strains and internal forces/moments obtained in Section 1, and after a proper integration by parts, it can be shown Eq.(2.2) yields[3]:

$$\begin{aligned} \delta U = \int_0^R [P_x' \delta u + P_y' \delta v + P_z' \delta w \\ + (M_y' - P_z) \delta \theta_y + (M_z' + P_y) \delta \theta_z \\ + (M_x' - Q_w'') \delta \phi] dx + b(U) \end{aligned} \quad (2.3)$$

Quantity	Order	Quantity	Order
$v/R, w/R$	$O(\varepsilon)$	h/Γ	$O(\varepsilon)$
u/R	$O(\varepsilon^2)$	ψ/L^2	$O(\varepsilon^2)$
x/R	$O(1)$	ϕ, θ_y, θ_z	$O(\varepsilon)$
$Y/R, Z/R, \eta/R, \zeta/R$	$O(\varepsilon)$	θ	$O(1)$
$c/R, t/R, \Gamma/R$	$O(\varepsilon)$	θ (only aerodyn. loads)	$O(\varepsilon)$
n/h	$O(1)$	$L \frac{d}{dx}, \Gamma \frac{d}{ds}, \frac{d}{\Omega dt}$	$O(1)$

Table (2.1): Orders of magnitude of various physical quantities

2.3 Kinetic Energy Contribution

The kinetic energy contribution to the total energy variation can be determined by considering the kinetic energy of a typical point on the beam wall. The result is [5]:

$$\begin{aligned} \delta T = \int_0^R [\bar{T}_u \delta u + (\bar{T}_v - \bar{T}_{v'}) \delta v + (\bar{T}_w - \bar{T}_{w'}) \delta w \\ + (\bar{T}_\phi - \bar{T}_{\phi'}) \delta \phi] dx + b(T) \end{aligned} \quad (2.4)$$

Assuming that the centre of mass is not offset from the elastic axis, and that the cross-section is symmetric about chord-wise principal axis, and denoting the beam mass/unit length as m , for an antisymmetric warp function ψ , in Eq.(2.4) one has:

$$\begin{aligned}
 \bar{T}_u &= m(\Omega^2 x + 2\Omega\dot{v}) \\
 \bar{T}_v &= m\Omega^2 v - m\ddot{v} - 2m\Omega\dot{u} \\
 \bar{T}_w &= -m\ddot{w} \\
 \bar{T}\phi &= -mk_m^2 \ddot{\phi} - m\Omega^2 (k_{m_2}^2 - k_{m_1}^2) \sin(\theta + \phi) \cos(\theta + \phi) \\
 \bar{T}_{v'} &= \bar{T}_{w'} = \bar{T}_{\phi'} = 0,
 \end{aligned} \tag{2.5}$$

where, θ is the pitch angle, mk_m^2 is the polar mass moment of inertia, and $mk_{m_1}^2$ and $mk_{m_2}^2$ are the principal mass moments of inertia of the cross-section.

2.4 Aerodynamic Contribution

All loads other than the elastic and inertial loads that act on the blade are non-conservative loads. In general, the non-conservative aerodynamic loads consist of L_u , L_v , L_w and M_ϕ , representing, respectively, the distributed loads that act in the x , y , and z directions, and the pitching moment about the elastic axis Fig.(1.1),. Then in reference to Eq.(2.1), one has

$$\delta W = \int_0^R [L_u \delta u + L_v \delta v + L_w \delta w + M_\phi \delta \phi] dx \tag{2.6}$$

For a first attempt in the modeling of the problem, hover conditions are considered in the present study. Greenberg's extension of Theodorsen's theory for a two-dimensional airfoil undergoing sinusoidal motion in pulsating incompressible flow has been used to determine the corresponding aerodynamic loads. In this approach, the aerodynamic forces are obtained using strip theory in which only the velocity component perpendicular to the deformed blade span-wise axis is assumed to influence the aerodynamic loads. Moreover, non-linear rate products such as $\dot{v}\dot{w}$, \dot{v}^2 and \dot{w}^2 as well as all terms of order $O(\varepsilon^3)$, except those that contribute to lead-lag or torsion damping, have been neglected. The resulting loads are [5]:

$$\begin{aligned}
 L_v &\cong \frac{\rho_\infty ac}{2} \left\{ v_i^2 - \Omega^2 x^2 \frac{c_{d_0}}{a} + \Omega x v_i (\theta + \phi) \right. \\
 &\quad \left. - [2\Omega x \frac{c_{d_0}}{a} - (\theta + \phi) v_i] \dot{v} + [2v_i + \Omega x (\theta + \phi)] \dot{w} \right\}
 \end{aligned}$$

$$\begin{aligned}
 L_w &\cong \frac{\rho_\infty ac}{2} \left\{ -\Omega x v_i + \Omega^2 x^2 (\theta + \phi + \int_0^x v' w'' dx) \right. \\
 &\quad \left. - \Omega^2 x v (\beta_{pc} + w') + \Omega^2 \frac{xc}{2} (\beta_{pc} + w') \right. \\
 &\quad \left. + [2\Omega x (\theta + \phi) - v_i] \dot{v} - \Omega x \dot{w} + \frac{3c}{4} \Omega x \dot{\phi} - \frac{c}{4} \dot{w} \right\} \\
 M_\phi &\cong \frac{\rho_\infty ac}{2} \left(\frac{c^2}{8} \Omega x \dot{\phi} \right)
 \end{aligned} \tag{2.7}$$

In Eq.(2.7) the following are defined:

$$\begin{aligned}
 \rho_\infty &= \text{air density (kg/m}^3\text{)}, \\
 a &= \text{airfoil lift curve slope (} 2\pi / \text{rad.)}, \\
 c &= \text{blade chord (m)}, \\
 c_{d_0} &= \text{airfoil profile drag coefficient}, \\
 \beta_{pc} &= \text{precone angle (assumed zero in this study)}.
 \end{aligned}$$

Moreover, the induced flow velocity, v_i is assumed to be steady and uniform along the rotor length. Its magnitude is taken to be equal to the value of non-uniform inflow obtained from blade element momentum theory at $x=0.75R$. Also, the blade angle at $x=0.75R$ is assumed to be equal to the blade collective pitch angle plus the equilibrium elastic twist ϕ_0 at $x=0.75R$. Then, using b blades with solidity $\sigma = bc / \pi R$, one has

$$\begin{aligned}
 v_i &= \text{sgn}[\theta + \phi_0(0.75R)] \frac{\pi\sigma}{8} \Omega R \\
 &\quad \cdot \left(\sqrt{1 + \frac{12}{\pi\sigma} |\theta + \phi_0(0.75LR)|} - 1 \right)
 \end{aligned} \tag{2.8}$$

2.5 Total Variational Equations

Substituting Eqs.(2.3-2.8) into Eq.(2.1) yields the total variational equations. For arbitrary admissible variations δu , δv , δw , $\delta\Phi$, $\delta\theta_y$, and $\delta\theta_z$, the coefficients of the variations in the resulting integrand as well as the boundary terms evaluated at $x=0$ and $x=R$ must vanish. This results in six non-linear partial differential equations in terms of u , v , w , ϕ , θ_y , and θ_z , plus the boundary conditions at the ends of the blade. The aerodynamic load L_u is neglected as

a higher order term. Moreover, the axial displacement u can be eliminated as an independent variable. Then one can obtain the final non-dimensional integro-partial differential equations of motion for the blade as:

δv equation:

$$\begin{aligned}
 & \left(\frac{\Lambda_{12}^2}{\Lambda_{11}} - \Lambda_{22}\right)\bar{v}'' + \left(\frac{\Lambda_{12}\Lambda_{13}}{\Lambda_{11}} - \Lambda_{23}\right)\bar{w}'' \\
 & + \left(\frac{\Lambda_{12}\Lambda_{15}}{\Lambda_{11}} - \Lambda_{25}\right)\theta_y'' + \left(\frac{\Lambda_{12}\Lambda_{16}}{\Lambda_{11}} - \Lambda_{26}\right)\theta_z'' \\
 & + \left(\frac{\Lambda_{12}\Lambda_{14}}{\Lambda_{11}} - \Lambda_{24}\right)\phi'' + \left(\frac{\Lambda_{12}\Lambda_{13}}{\Lambda_{11}} - \Lambda_{23}\right)\theta_y' \\
 & + \left(\frac{\Lambda_{12}^2}{\Lambda_{11}} - \Lambda_{22}\right)\theta_z' + \ddot{\bar{v}} - \bar{v} + \frac{\gamma}{6} \left\{ \left[\frac{2c_{d_0}}{a} \bar{x} - (\theta + \phi)\bar{v}_i \right] \dot{\bar{v}} \right. \\
 & \left. - [2\bar{v}_i + \bar{x}(\theta + \phi)]\dot{\bar{w}} - \bar{x}\bar{v}_i\dot{\phi} \right\} - \frac{2\Lambda_{13}}{\Lambda_{11}} \dot{\bar{w}} - 2\frac{\Lambda_{15}}{\Lambda_{11}} \dot{\theta}_y \\
 & - 2\frac{\Lambda_{16}}{\Lambda_{11}} \dot{\theta}_z - 2\frac{\Lambda_{14}}{\Lambda_{11}} \dot{\phi} - 2\frac{\Lambda_{13}}{\Lambda_{11}} \int \dot{\theta}_y d\bar{x} + 2\frac{\Lambda_{12}}{\Lambda_{11}} \int \dot{\theta}_z d\bar{x} \\
 & = -\frac{\Lambda_{12}}{\Lambda_{11}} \bar{x} + \frac{\gamma}{6} (\bar{v}_i^2 - \frac{c_{d_0}}{a} \bar{x}^2 + \bar{x}\bar{v}_i\theta) + \frac{\Lambda_{12}}{\Lambda_{11}} (\bar{P}_x^a)' - (\bar{P}_y^a)'
 \end{aligned} \tag{2.9.1}$$

δw equation:

$$\begin{aligned}
 & \left(\frac{\Lambda_{13}\Lambda_{12}}{\Lambda_{11}} - \Lambda_{23}\right)\bar{v}'' + \left(\frac{\Lambda_{13}^2}{\Lambda_{11}} - \Lambda_{33}\right)\bar{w}'' \\
 & + \left(\frac{\Lambda_{13}\Lambda_{15}}{\Lambda_{11}} - \Lambda_{35}\right)\theta_y'' + \left(\frac{\Lambda_{13}\Lambda_{16}}{\Lambda_{11}} - \Lambda_{36}\right)\theta_z'' \\
 & + \left(\frac{\Lambda_{13}\Lambda_{14}}{\Lambda_{11}} - \Lambda_{34}\right)\phi'' + \left(\frac{\Lambda_{13}^2}{\Lambda_{11}} - \Lambda_{33}\right)\theta_y' \\
 & - \left(\frac{\Lambda_{13}\Lambda_{12}}{\Lambda_{11}} - \Lambda_{23}\right)\theta_z' + 2\frac{\Lambda_{13}}{\Lambda_{11}} \dot{\bar{v}} + \left(\frac{\gamma\bar{c}}{24} + 1\right)\ddot{\bar{w}} \\
 & + \frac{\gamma}{2} \left\{ -\bar{x}^2(\phi + \int \bar{v}'\bar{w}' d\bar{x}) + \bar{x}\bar{v}\bar{w}' - \frac{\bar{c}}{2}\bar{x}\bar{w}' \right. \\
 & \left. - [2\bar{x}(\theta + \phi) - \bar{v}_i]\dot{\bar{v}} + \bar{x}\dot{\bar{w}} - \frac{3}{4}\bar{c}\bar{x}\dot{\phi} \right\} \\
 & = -\frac{\Lambda_{13}}{\Lambda_{11}} \bar{x} - \frac{\gamma}{6} \bar{x}[\bar{v}_i - \bar{x}\theta] + \frac{\Lambda_{13}}{\Lambda_{11}} (\bar{P}_x^a)' - (\bar{P}_z^a)'
 \end{aligned} \tag{2.9.2}$$

$\delta\phi$ equation:

$$\begin{aligned}
 & \Lambda_{27}\bar{v}'' + \Lambda_{37}\bar{w}'' + \left(\frac{\Lambda_{14}\Lambda_{12}}{\Lambda_{11}} - \Lambda_{24}\right)\bar{v}'' \\
 & + \left(\frac{\Lambda_{14}\Lambda_{13}}{\Lambda_{11}} - \Lambda_{34}\right)\bar{w}'' + \left(\frac{\Lambda_{14}\Lambda_{15}}{\Lambda_{11}} - \Lambda_{45} + \Lambda_{37}\right)\theta_y'' \\
 & + \left(\frac{\Lambda_{14}\Lambda_{16}}{\Lambda_{11}} - \Lambda_{46} - \Lambda_{27}\right)\theta_z'' + \left(\frac{\Lambda_{14}^2}{\Lambda_{11}} - \Lambda_{44}\right)\phi'' \\
 & + \left(\frac{\Lambda_{14}\Lambda_{13}}{\Lambda_{11}} - \Lambda_{34}\right)\theta_y' + \left(-\frac{\Lambda_{14}\Lambda_{12}}{\Lambda_{11}} + \Lambda_{24}\right)\theta_z' \\
 & + 2\frac{\Lambda_{14}}{\Lambda_{11}} \dot{\bar{v}} + \frac{\gamma\bar{c}^2}{48} \bar{x}\dot{\phi} + \mu_2^2 \ddot{\phi} + (\mu_2^2 - \mu_1^2)\phi \cos 2\theta \\
 & = -\frac{\Lambda_{14}}{\Lambda_{11}} \bar{x} - \frac{1}{2}(\mu_2^2 - \mu_1^2)\sin 2\theta + \frac{\Lambda_{14}}{\Lambda_{11}} (\bar{P}_x^a)' - (\bar{M}_x^a)' + (\bar{Q}_w^a)'
 \end{aligned} \tag{2.9.3}$$

$\delta\theta_y$ equation:

$$\begin{aligned}
 & \Lambda_{25}\bar{v}'' + \Lambda_{35}\bar{w}'' + \left(\frac{\Lambda_{13}\Lambda_{12}}{\Lambda_{11}} - \Lambda_{23}\right)\bar{v}'' + \left(\frac{\Lambda_{13}^2}{\Lambda_{11}} - \Lambda_{33}\right)\bar{w}'' \\
 & + \frac{\Lambda_{13}\Lambda_{15}}{\Lambda_{11}} \theta_y'' + \left(\frac{\Lambda_{13}\Lambda_{16}}{\Lambda_{11}} - \Lambda_{25} - \Lambda_{36}\right)\theta_z'' \\
 & + \left(\frac{\Lambda_{13}\Lambda_{14}}{\Lambda_{11}} - \Lambda_{34}\right)\phi'' + \left(\frac{\Lambda_{13}^2}{\Lambda_{11}} - \Lambda_{33}\right)\theta_y' \\
 & + \left(-\frac{\Lambda_{13}\Lambda_{12}}{\Lambda_{11}} + \Lambda_{23}\right)\theta_z' + 2\frac{\Lambda_{13}}{\Lambda_{11}} \dot{\bar{v}} \\
 & = -\frac{\Lambda_{13}}{\Lambda_{11}} \bar{x} + \frac{\Lambda_{13}}{\Lambda_{11}} (\bar{P}_x^a)' - (\bar{P}_z^a)' + (\bar{M}_y^a)'
 \end{aligned} \tag{2.9.4}$$

$\delta\theta_z$ equation:

$$\begin{aligned}
 & \Lambda_{26}\bar{v}'' + \Lambda_{36}\bar{w}'' + \left(-\frac{\Lambda_{12}^2}{\Lambda_{11}} + \Lambda_{22}\right)\bar{v}'' \\
 & + \left(-\frac{\Lambda_{12}\Lambda_{13}}{\Lambda_{11}} + \Lambda_{23}\right)\bar{w}'' + \left(-\frac{\Lambda_{12}\Lambda_{15}}{\Lambda_{11}} + \Lambda_{25} + \Lambda_{36}\right)\theta_y'' \\
 & - \frac{\Lambda_{12}\Lambda_{16}}{\Lambda_{11}} \theta_z'' + \left(-\frac{\Lambda_{12}\Lambda_{14}}{\Lambda_{11}} + \Lambda_{24}\right)\phi'' \\
 & + \left(-\frac{\Lambda_{12}\Lambda_{13}}{\Lambda_{11}} + \Lambda_{23}\right)\theta_y' + \left(\frac{\Lambda_{12}^2}{\Lambda_{11}} - \Lambda_{22}\right)\theta_z' - 2\frac{\Lambda_{12}}{\Lambda_{11}} \dot{\bar{v}} \\
 & = \frac{\Lambda_{12}}{\Lambda_{11}} \bar{x} - \frac{\Lambda_{12}}{\Lambda_{11}} (\bar{P}_x^a)' + (\bar{P}_y^a)' + (\bar{M}_z^a)'
 \end{aligned} \tag{2.9.5}$$

3. Stability Analysis

3.1 Perturbation Equations

The necessary equations of perturbation that can be used in the aeroelastic stability analysis of the blade can be obtained from Eqs.(2.9.1-2.9.5). These non-linear, variable coefficient, integro-partial differential equations can be solved by Galerkin's method [3,5]. To this end, the displacements are expanded as a series of products of generalised modal coordinates and mode shapes:

$$\begin{aligned} \bar{v} &= \sum_{j=1}^N V_j(\Psi) \varphi_j^v(\bar{x}), & \bar{w} &= \sum_{j=1}^N W_j(\Psi) \varphi_j^w(\bar{x}), \\ \phi &= \sum_{j=1}^N \Phi_j(\Psi) \varphi_j(\bar{x}), & \theta_y &= \sum_{j=1}^N \Theta_j^y(\Psi) \varphi_j^y(\bar{x}), \\ \theta_z &= \sum_{j=1}^N \Theta_j^z(\Psi) \varphi_j^z(\bar{x}) \end{aligned} \quad (3.1)$$

where $\Psi = \Omega t$ is the azimuth angle, and $V_j(\psi)$, $W_j(\psi)$, $\Phi_j(\psi)$, $\Theta_j^y(\psi)$ and $\Theta_j^z(\psi)$ are the generalised modal co-ordinates. The uncoupled mode shapes of a standard non-rotating, uniform cantilever beam may be used for $\varphi_j^v(\bar{x})$, $\varphi_j^w(\bar{x})$ and $\varphi_j(\bar{x})$ as suggested in [3,4,5]. Moreover, the actuation terms in Eqs.(2.9), also, can each be expressed as a series expansion:

$$\begin{aligned} \bar{P}_x^a &= E(\psi) \sum_{j=1}^N p_j^x(\bar{x}), & \bar{P}_y^a &= E(\psi) \sum_{j=1}^N p_j^y(\bar{x}), \\ \bar{P}_z^a &= E(\psi) \sum_{j=1}^N p_j^z(\bar{x}), & \bar{M}_x^a &= E(\psi) \sum_{j=1}^N m_j^x(\bar{x}), \\ \bar{M}_y^a &= E(\psi) \sum_{j=1}^N m_j^y(\bar{x}), & \bar{M}_z^a &= E(\psi) \sum_{j=1}^N m_j^z(\bar{x}), \\ \bar{Q}_w^a &= E(\psi) \sum_{j=1}^N q_j^w(\bar{x}), \end{aligned} \quad (3.2)$$

where, $E(\psi)$ is the applied electric field, and, $p_j^x(\bar{x})$, $p_j^y(\bar{x})$, $p_j^z(\bar{x})$, $m_j^x(\bar{x})$, $m_j^y(\bar{x})$, $m_j^z(\bar{x})$ and $q_j^w(\bar{x})$ are the effect of the respective actuation on each mode shape due to material

properties and physical construction of the integrated active fibres. The influence of j -th actuation term can be determined as the ratio of the j -th mode shape over the sum of the mode shapes. Using the series expansions given in Eqs.(3.1), the governing equations of motion (2.9) can, first, be reduced to a set of $5N$ ordinary differential equations in terms of generalised co-ordinates. Next, small perturbation motions about the equilibrium operating conditions are considered by expressing each time-dependent generalized coordinate as the sum of a steady equilibrium quantity that defines the corresponding equilibrium deflection, and a small unsteady perturbation quantity, i.e.,

$$\begin{aligned} V_j(\Psi) &= V_{0j} + \Delta V_j(\Psi), & W_j(\Psi) &= W_{0j} + \Delta W_j(\Psi), \\ \Phi_j(\Psi) &= \Phi_{0j} + \Delta \Phi_j(\Psi), & \Theta_j^y(\Psi) &= \Theta_{0j}^y + \Delta \Theta_j^y(\Psi), \\ \Theta_j^z(\Psi) &= \Theta_{0j}^z + \Delta \Theta_j^z(\Psi) \end{aligned} \quad (3.3)$$

Two sets of equations can be obtained by incorporating Eqs.(3.3) into Eqs.(2.9). The first set will be the result of substituting the steady equilibrium quantities into Eqs.(2.9). This will yield $5N$ non-linear algebraic equations in V_{0j} , W_{0j} , Φ_{0j} , Θ_{0j}^y , and Θ_{0j}^z that can be solved by any standard non-linear technique such as Newton-Raphson or Least Mean Square method. The second set of equations can be obtained by substituting Eqs.(3.3) into Eqs.(2.9), subtracting from the resulting system the first system that was obtained from equilibrium quantities, and neglecting all the higher order terms in perturbation quantities. This will yield a system of linearized perturbation equations with coefficients that are functions of steady equilibrium quantities as determined from the first set. These perturbation equations constitute a set of linear, homogeneous, constant coefficient, ordinary differential equations that define the unsteady blade motion near the equilibrium operating condition, and therefore, can be used to determine the stability of this motion. To this end, defining a vector of unknowns

$$\mathbf{X}^T = [\Delta V_j \quad \Delta W_j \quad \Delta \Phi_j \quad \Delta \Theta_j^y \quad \Delta \Theta_j^z] \quad (3.4)$$

the perturbation equations will have the general form of

$$\mathbf{M}\ddot{\mathbf{X}} + \mathbf{C}_t\dot{\mathbf{X}} + \mathbf{K}_t\mathbf{X} + \mathbf{F}\Delta E = \mathbf{0} \quad (3.5)$$

where the subscript t denotes the total matrices that are composed of gyroscopic, aerodynamic and structural contributions:

$$\mathbf{C}_t = \mathbf{C}_g + \mathbf{C}_a, \quad \mathbf{K}_t = \mathbf{K}_s + \mathbf{K}_a. \quad (3.6)$$

The set of Eqs.(3.6) may be rewritten as

$$\begin{bmatrix} \dot{\mathbf{X}} \\ \ddot{\mathbf{X}} \end{bmatrix} = \begin{bmatrix} \mathbf{0} & \mathbf{I} \\ -\mathbf{M}^{-1}\mathbf{K}_t & -\mathbf{M}^{-1}\mathbf{C}_t \end{bmatrix} \begin{bmatrix} \mathbf{X} \\ \dot{\mathbf{X}} \end{bmatrix} + \begin{bmatrix} \mathbf{0} \\ -\mathbf{M}^{-1}\mathbf{F} \end{bmatrix} \Delta E = \mathbf{A} \begin{bmatrix} \mathbf{X} \\ \dot{\mathbf{X}} \end{bmatrix} + \mathbf{B}\Delta E \quad (3.7)$$

In this form, the eigenvalues of the matrix \mathbf{A} determine the stability of the motion under consideration. Moreover, the input control vector \mathbf{B} can therefore be used for vibration control.

4 Conclusions and Recommendations

Basically, this report is comprised of two parts. The first part deals with providing an analytical structural model for a single-cell, thin-walled composite rotor blade with fully integrated active fibres. This model is based on a linear formulation using macro-mechanics of composite plate theory. It considers a displacement field that accounts for axial, torsional, lead-lag and flap actions in the blade. The resulting beam stiffness matrix can represent coupling between various actions such as axial, torsional, bending and shear in the blade. In the second part of the report, a set of non-linear dynamic equations of motion has been developed for a hingeless rotor blade using the structural model presented in the first part. It has been shown how this dynamic model can be used in aeroelastic stability investigation and dynamic control and analysis of the rotor. Application of this modelling to a typical

composite rotor blade and simulation of the corresponding results will be the subject of a subsequent paper.

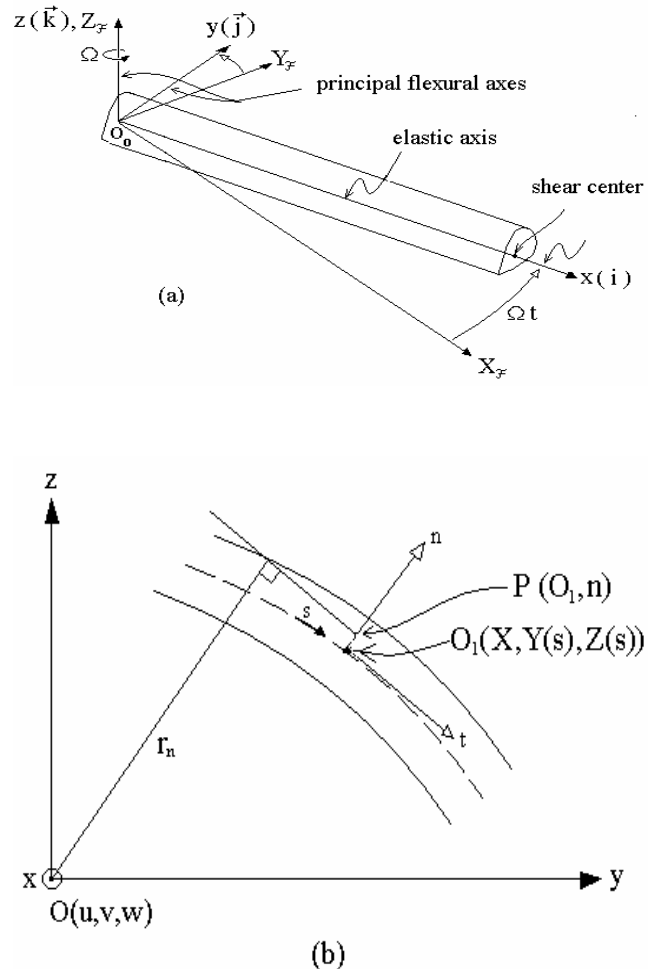


Figure 1.1: Rotor blade co-ordinate systems

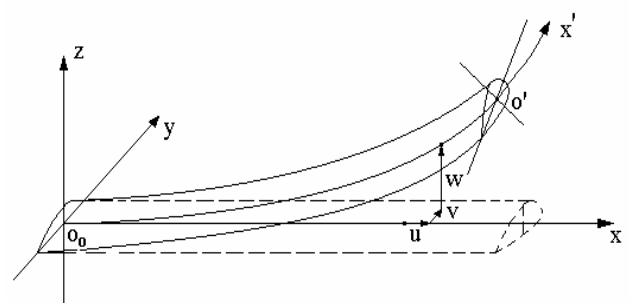


Figure 1.2: Rotor blade displacement

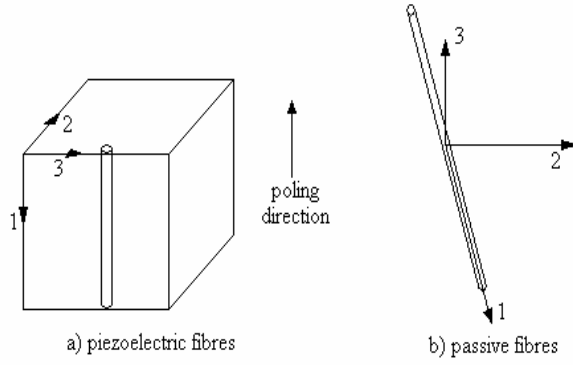
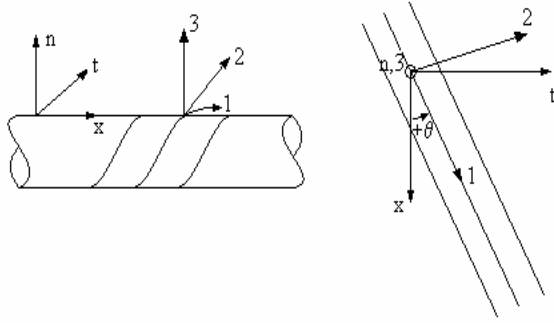


Figure (1.3): Material axes for active and passive



Figure(1.4): Principal material axes vs. structural axes

Acknowledgement

This work was carried out at the Institut für Strukturmechanik in the German Aerospace Centre (DLR) during the author's sabbatical leave in 2000-01.

Appendix

Stiffness coefficients K_{ij} for the normal internal force N :

$$\begin{aligned}
 K_{11} &= \int_{\Gamma} \bar{A}_{11} ds, & K_{12} &= \int_{\Gamma} \bar{A}_{12} Y_{,s} ds, & K_{13} &= \int_{\Gamma} \bar{A}_{12} Z_{,s} ds, \\
 K_{14} &= -2 \int_{\Gamma} \bar{A}_{12} \left(\frac{A\alpha}{\Gamma} \right) ds, & K_{15} &= \int_{\Gamma} (\bar{A}_{11} Z + \bar{A}_{13} Y_{,s}) ds, \\
 K_{16} &= \int_{\Gamma} (\bar{A}_{13} Z_{,s} - \bar{A}_{11} Y) ds, \\
 K_{17} &= \int_{\Gamma} \bar{A}_{11} \psi ds
 \end{aligned} \tag{A.1}$$

The applied force vector:

$$[\mathbf{F}^a]^T = [P_x^a \quad P_y^a \quad P_z^a \quad M_x^a \quad M_y^a \quad M_z^a \quad Q_w^a]$$

where,

$$\begin{aligned}
 P_x^a &= \int_{\Gamma} \bar{N}_{xx}^a ds, & P_y^a &= \int_{\Gamma} \bar{N}_{xx}^a Y_{,s} ds, & P_z^a &= \int_{\Gamma} \bar{N}_{xx}^a Z_{,s} ds, \\
 M_x^a &= -2 \int_{\Gamma} \bar{N}_{xx}^a \left(\frac{A\alpha}{\Gamma} \right) ds, & M_y^a &= \int_{\Gamma} (\bar{N}_{xx}^a Z + \bar{M}_{xx}^a Y_{,s}) ds, \\
 M_z^a &= \int_{\Gamma} (-\bar{N}_{xx}^a Y + \bar{M}_{xx}^a Z_{,s}) ds, \\
 Q_w^a &= \int_{\Gamma} \bar{N}_{xx}^a \psi ds.
 \end{aligned} \tag{A.2}$$

References

- [1] Hodges, D.H. Review of composite rotor blade modelling, *AIAA Journal*, Vol. 28, No.3, pp.561-565, 1990.
- [2] Jones, R.M. *Mechanics of Composite Materials*. McGraw-Hill, 1975.
- [3] Afagh, F.F. Modelling of helicopter rotor blades with integrated active fibres for vibration control and aeroelastic analysis, *Report No. DLR IB 131-2001/38*, 2001.
- [4] Hodges, D.H. and Dowell, E.H. Non-linear equations of motion for the elastic bending and torsion of twisted non-uniform rotor blades, *Report No.: NASA TN D-7818*, 1974.
- [5] Hodges, D.H. and Ormiston, R.A. Stability of elastic bending and torsion of uniform cantilever rotor blades in hover with variable structural coupling, *Report No.: NASA TN D-8192*, 1976.